Temperature Compensated Tactile Sensing using MOSFET with P(VDF-TrFE)/$BaTiO_3$ Capacitor as Extended Gate

Shoubhik Gupta, Dhayalan Shakthivel, Leandro Lorenzelli, Ravinder Dahiya

Abstract—This work presents Poly(vinylidene fluoride – trifluoroethylene))/Barium Titanate (P(VDF-TrFE)-BT) nanocomposite based touch sensors tightly coupled with MOSFET devices in extended gate configuration. The P(VDF-TrFE)-BT nanocomposite exploits the distinct piezo and pyroelectric properties of P(VDF-TrFE) polymer matrix and BT fillers to suppress the temperature response when force and temperature are varied simultaneously. The reasons for this unique feature have been established through structural and electrical characterization of nanocomposite. The proposed touch sensor was tested over a wide range of force/pressure (0-4N)/(0-364 Pa) and temperature (26-70ºC) with almost linear response. The sensitivity towards force/pressure and temperature sensor are 670 mV/N/7.36 mV/Pa and 15.34 mV/ºC respectively. With this modified touch sensing capability, the proposed sensors will open new direction for tactile sensing in robotic applications.

***Index Terms*— multimodal tactile sensor, nanocomposite, extended gate, MOSFETs, P(VDF-TrFE), e-skin**

I. Introduction

Tactile sensing has attracted significant attention recently for safe and interactive robots as well as prosthesis with touch feelings [1-4]. For amputees that have lost their hands, one of the biggest sources of frustration is the inability to sense what they are touching while using prosthetic devices. Likewise, realizing the vision of future manufacturing with robots working side-by-side with skilled workers or robots helping elderly at home will be difficult without safe physical interaction and hence the tactile sensing [5]. As a result, there is a considerable interest to cover parts of robot's body with tactile sensors or tactile or electronic skin (e-skin) [6]. The effective use of e-skin relies on tactile sensors that can [7] (a) sense multiple touch parameters (e. g. temperature, pressure, etc.), (b) conform to curvy surfaces, (c) work on negligible or no power, and (d) handle the large data. This wish-list is in addition to the traditional requirements related to sensors, such as excellent sensitivity, and fast response etc. [3]

While the work on flexible or conformable e-skin [7, 8] energy-autonomous tactile skin [6] and data handling in e-skin [9] has gained pace, the research on multimodal touch sensors (i.e. sensors capable of measuring multiple parameters) is yet to gather the momentum. This is partly attributed to the challenges in terms of getting the materials that are suitable for multimodal tactile sensing [4]. Towards this end, materials such as P(VDF-TrFE) have been explored. In addition to being flexible and piezoelectric, these polymers are also pyroelectric [10]. This means the touch sensors from P(VDF-TrFE) can respond to variations in force and temperature and hence it is possible to have multimodal touch sensors. However, in P(VDF-TrFE) both these effects exist simultaneously and hence it is difficult to separate the response due to pyro and piezoelectric effects [11]. As a result, P(VDF-TrFE) based force sensors either require additional strategy to compensate the effect of variation in temperature or require operation under constant temperature [12, 13]. Likewise, the temperature sensors from P(VDF-TrFE) require additional strategy to compensate the effect of variation in force. In order to completely nullify the effect of temperature, a temperature compensation methodology comprising a negative temperature coefficient thermistor with the temperature characteristics of a piezoelectric material has also been reported [14]. It can also be achieved by representing the sensor signals through the Hilbert transform and then employs an ordinary least square (OLS) algorithm for estimating the change in amplitude and phase-shift due to temperature [15].

The issue is addressed here by using poly(vinylidene fluoride-trifluoroethylene))/Barium Titanate (P(VDF-TrFE)/$BaTiO_3$ or P(VDF-TrFE)-BT)) nanocomposite to develop the tactile sensing devices. This paper extends the work presented at 2017 IEEE Sensors Conference, where we reported the capacitive structure based on P(VDF-TrFE)-BT nanocomposite [16]. Building on that work, we present here the tactile sensing devices made from a FET (Field Effect Transistor) connected with P(VDF-TrFE)-BT nanocomposite capacitor. The capacitor, which forms the sensing part, is connected with FET in an extended gate configuration (Fig.1). The unique combination of P(VDF-TrFE) and BT allows the tactile sensing device to sense temperature and force without the typical compensation requirement as discussed above. The touch sensor device has been tested over a wide range of force (0-4N) and temperature (26 -70ºC) and achieved sensitivity are

An earlier version of this paper was presented at the IEEE Sensors Conference, 2017 was published in its proceedings
[http://ieeexplore.ieee.org/abstract/document/8234096/]
This work was supported in part by the EPSRC Engineering Fellowship for Growth - PRINTSKIN (EP/M002527/1) and European Commission under Grant Agreements PITN-GA-2012-317488-CONTEST.

S. Gupta, D. Shakthivel and R. Dahiya are with the Bendable Electronics and Sensing Technologies (BEST) group in School of Engineering, University of Glasgow, Glasgow, G12 8QQ, United Kingdom.
(e-mail: Ravinder.Dahiya@glasgow.ac.uk).
L. Lorenzelli is with Microsystems Technology Research Unit, Fondazione Bruno Kessler, 38123, Trento, Italy.

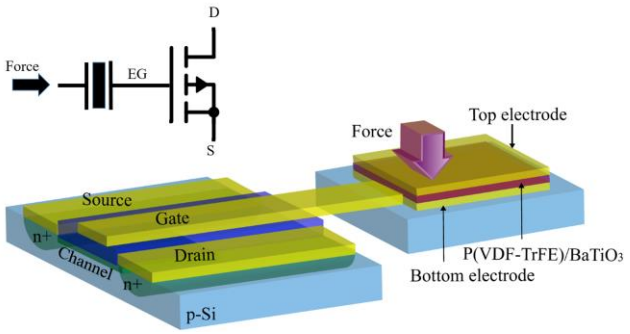

Figure 1: Illustration of P(VDF-TrFE)-BT nanocomposite coupled to a MOSFET in extended gate configuration and its symbolic representation.

Table I: Various works reported in literature using PVDF and BaTiO3 based composite.

Polymer	Filler	Application	Figure of Merit	Ref
PVDF	BT	Energy harvesting	Output power: 25 µW	[17]
PVDF	BT	Energy storage	Energy density: 18.8J cm−3	[18]
PVDF-HFP	BT	Nano generator	Output voltage: 75 V @0.23 MPa	[19]
PVDF	BT, Ag	EMI shielding	Shielding effectiveness: 26 dB	[20]
PVDF	BT	Flow Sensor	15.8 nW at 125.7 m/s.	[21]
Epoxy	BT/PMN-PT	Capacitor	Capacitance density: 50 nF/cm2	[22]

670 mV/N and 15.34 mV/^{o}C respectively.

This paper is organized as follows: Section II provides a brief description related to the material selection and the state-of-art related to 0-3 nanocomposite. Section III presents the fabrication and characterization of the two main constituents (i.e. sensing part and the MOSFET) of tactile sensing devices. The electrical and electromechanical performance of tactile sensing device are presented in Section IV. Finally, the paper is concluded in Section V.

II. Material Selection

Suitable selection of inclusions, polymer and their volume ratio could allow the fabrication of new materials with tailored properties with considerable potential in sensor applications. For example, composites of BT and polyvinylidenefluoride (PVDF) have been explored for energy storage because it combines excellent dielectric properties of the PVDF polymer with the high permittivity of BT ceramics in a broad frequency range [17, 18, 23, 24]. Composites with inclusions of inorganic fillers such as nanoparticles, nanowires embedded in polymer matrix have been used for various applications summarized in Table I [25].

With ferroelectric ceramics (e.g. BT, lead titanate (PT) etc.) as inclusions the composites can offer promising solutions for multifunctional touch sensing as they combine the high pyroelectric and piezoelectric coefficients of the ceramic with the good mechanical properties (e.g. flexibility) of the polymer. The polymer could be a simple elastomer such as PDMS, PVC or active polymer such as PVDF and its copolymer etc. [4, 26].

In the event when both the inclusions and polymer matrix are ferroelectric (e.g. matrix of PVDF or its copolymer P(VDF-TrFE)), then the poling state of the matrix could be tailored to get an additional degree of freedom. For example, by polarizing only the polymer matrix (Fig. 2(a)) or only the inclusions (i.e. BT in P(VDF-TrFE)-BT nanocomposite) (Fig. 2(b)) it is possible to tailor the effective pyroelectric and piezoelectric coefficients of the composite. When both constituents (i.e. fillers and polymer matrix) are polarized simultaneously in either opposite direction (Fig. 2(c)) or the same direction (Fig. 2(d)), the overall piezoelectric or pyroelectric effect may be strengthened. This depends on the piezoelectric and pyroelectric coefficients of the constituents. For example, in P(VDF-TrFE)-BT nanocomposite, the piezoelectric coefficient of BT has positive polarity and that of P(VDF-TrFE) is negative. The opposite polarity of these constituents (Fig. 2(c)) lead to strengthening of piezoelectric coefficient d_{33} when they are poled in opposite direction. Likewise, when they are polarized in same direction (Fig. 2(d)), the piezoelectric coefficient will be weakened, but the pyroelectric effect will get stronger. This feature has been exploited in past, with PT and P(VDF–TrFE) composite, to compensate the piezoelectric or pyroelectric effect [27]. However, this unique property has been exploited in this paper to develop a touch-sensing device having capability to respond to either force or temperature. There have been reports of using combination of PZT and PVDF, where by defining the poling condition, one effect is suppressed in comparison to other [28, 29]. However, as the family of lead based piezoelectric materials are now facing summons due to their toxicity, environmental compatibility and possible danger during fabrication, usage and disposal; lead-free piezoelectric material are researched. So, instead of using PZT, which is undesirable of tactile skin application due to presence of lead, we have used BT inclusions in P(VDF-TrFE). BT-PVDF nanocomposites are emerging as good choice for sensor applications due to their biocompatibility, convenient fabrication process, low cost, and tuneable properties [30-32]. Although the piezoelectric coefficient of BaTiO3 is lesser than that of PZT as can be seen from Table II, but its superiority over PVDF and environmental friendly nature makes it an attractive choice for the applications involving close human interaction such as tactile sensing.

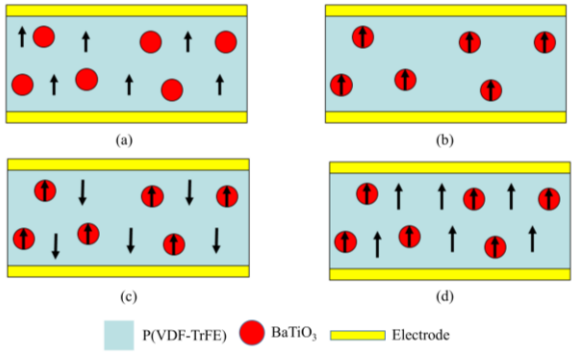

Figure 2: The polarization state in (a) poled P(VDF-TrFE); (b) poled BT; (c) P(VDF-TrFE) and BT poled in opposite direction leading to strengthening of piezoelectric effect; (d) P(VDF-TrFE) and BT poled in the same direction to lead to strengthening of pyroelectric effect.

Table II: Various coefficients associated with PZT, $BaTiO_3$ and P(VDF-TrFE)			
	PZT [33, 34]	BaTiO3[35, 36]	P(VDF-TrFE) [37]
Piezoelectric charge constant, d_{33} *(pC/N)*	374	191	22
Piezoelectric stress constant, e_{33} (C/m^2)	15.8	11.6	-0.165
Piezoelectric voltage constant, $g_{33}(10^{-8}V.m/N)$	24.9	11.4	-0.38
Piezoelectric stiffness constant, h_{33} (10^8 V/m)	21.4	9.2	-4.3
Dielectric constant, ε_{33}	1700	1680	9-12
Electromechanical coupling coefficient, k_{33}	0.7	0.49	0.15
Pyroelectric coefficient, p ($\mu C/m^2K$)	74	-20 ±2	-20 ±4

III. Fabrication And Characterization

A. Tactile Sensing Device fabrication

In the first step, the BT nanoparticles (average size of about 100 nm) from Sigma Aldrich were dispersed in Methyl Ethyl Ketone (MEK) solvent using probe sonication. This was followed by the dissolution of 70/30 P(VDF-TrFE) pellets (from Piezotech) at elevated temperature (80ºC) with magnetic stirring. This was done to prevent the agglomeration of nanoparticles in viscous P(VDF-TrFE) solution. The nanocomposite is then placed in sonication bath for 1 hour before spin coating. Polyimide film (from Dupont) was then used as the flexible substrate to realize the touch sensitive layer from P(VDF-TrFE)-BT nanocomposite. The PI film was cleaned via series of ultrasonic baths and then a 100 nm metal (Al) layer was evaporated to obtain the bottom electrode. Then the nanocomposite was spin coated in two steps of 500 rpm for 10 s followed by 1000 rpm for 30 s, to ensure uniform spread of nanocomposite and uniform thickness of sample. The film was then annealed in nitrogen ambient for an hour at 140ºC. At this temperature, the viscosity of nanocomposite is low enough to allow the motion of conformers without deformation of crystal structure. Since 140ºC is more than α relaxation temperature, the tendency of crystallization to β phase is considerably higher. After annealing the thickness of the film was measured as 4-µm. Following this, 10 nm/50 nm nichrome/gold were evaporated through hard mask to realize top electrode. Finally, the PI substrate was released from the carrier wafer and taxel were separated for further characterization. The spin coating approach resulted in thickness which is an order of magnitude lesser than that obtained by hot melting process[29], and thus require much less poling voltage.

The MOSFET used in this work is same as the one described elsewhere [11]. With the aspect ratio of 273, it was fabricated using non-standard 4-µm CMOS technology with n-MOSFET in p-well. The adopted technology ensures high mobility FET with stable performance, in comparison to sensor comprised of organic FET and thin film transistors [12, 29]. The fabrication starts with implantation for p-well using boron in n-type wafer.

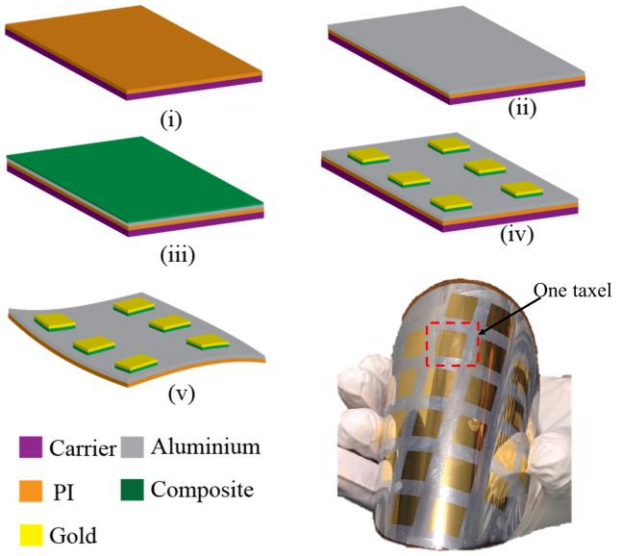

Figure 3: Fabrication steps adopted for realizing the sensing structure.

500 nm thick field oxide was grown by wet oxidation, followed

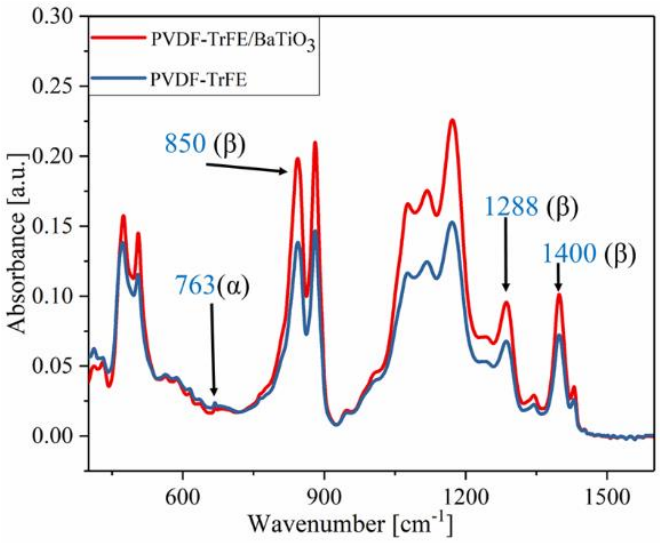

Figure 4: FTIR spectra of P(VDF-TrFE) and P(VDF-TrFE)-BT nanocomposite showing the characteristic peaks of polar phases.

by defining and implanting source-drain region using phosphorus and arsenic dopants. A stack of silicon nitride (Si_3N_4) and silicon dioxide (SiO_2) with effective oxide thickness of 45 nm was used as gate dielectric. Afterwards, 500 nm thick Low-Temperature SiO_2 was deposited for electrical insulation of device and contact holes to the diodes, well and gate region were opened. Finally, aluminum was deposited and patterned to realize the interconnection scheme.

The sensing layer and MOSFET were then connected in extended gate configuration to realize the sensor.

C. Spectroscopy Analysis

The molecular structure of P(VDF-TrFE)-BT nanocomposite film was analyzed using FTIR (Fig. 4) and Raman (Fig. 5) spectroscopy. These studies mainly focused on the influence of

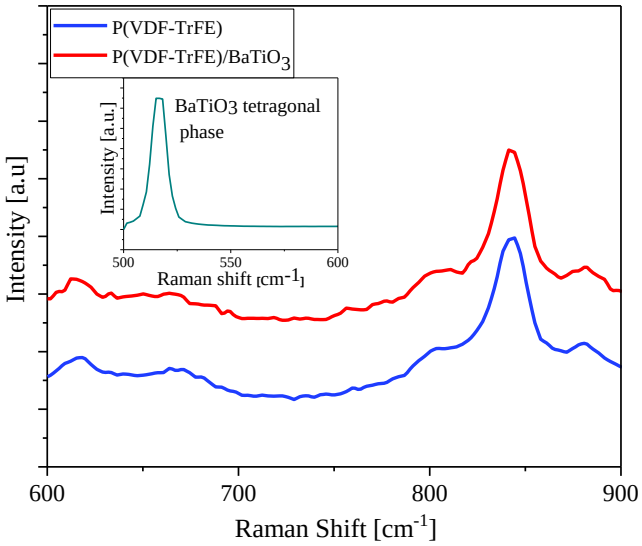

Figure 5: Raman spectra of P(VDF-TrFE) and P(VDF-TrFE)-BT nanocomposite showing the β peak enhancement. Inset shows the tetragonal phase of BT.

BT nanoparticles in the nanocomposite structure. The enhancement of β-phase with addition of BT in the matrix is evident from the FTIR and Raman spectra. The FTIR spectrum was recorded in the frequency range of 400-1600 cm^{-1}, where the characteristic vibration bands of P(VDF-TrFE) emerge. Analysis of these vibration bands helps us to understand the polar β-phase of P(VDF-TrFE) polymer. Three characteristic peaks (i.e. 850, 1288 and 1400 cm^{-1}) shown in Fig. 4 depict various bond stretching associated with ferroelectric β-phase of P(VDF-TrFE). For example, peak at 1288 cm^{-1} corresponds to CF_2 asymmetric stretching and C—C symmetric stretching. The bonding in β-phase are polar in nature and could be influenced by external electric field [38]. Additionally, the spectrum clearly distinguishes the dominant polar and weak nonpolar phases. A deeply diminished non-polar α-phase appears close to 763cm^{-1} compared to the intense β- phase at 850 cm^{-1}. Additionally, the peak intensity of β-phase is higher with BT inclusion (Fig.4). This observation verifies escalation of β-phase in the composite upon addition of BT nanoparticles in P(VDF-TrFE) matrix. BT nanoparticles are expected to be active sites for the β-phase formation in P(VDF-TrFE) matrix. The underlying mechanism of P(VDF-TrFE)-BT interface characteristics is explained elsewhere [38]. In brief, the negatively charged fluorine in P(VDF-TrFE) matrix can readily combined with positively charged BT. Lattice vacancies in BT keeps it positively charged. The introduction of fluorine in octahedron structure of BT decreases the interface and space charges. This leads to increase in the dielectric constant of the nanocomposite as the electric dipoles can move easily without much hindrance from space and interface charge. The additional Raman spectroscopy analysis (Fig. 5) confirms the presence of β phase in the nanocomposite. The inset in Fig. 5 shows the Raman spectrum for a short range of 500-600 cm^{-1} that reveals the tetragonal phase of BT NPs. This verifies the

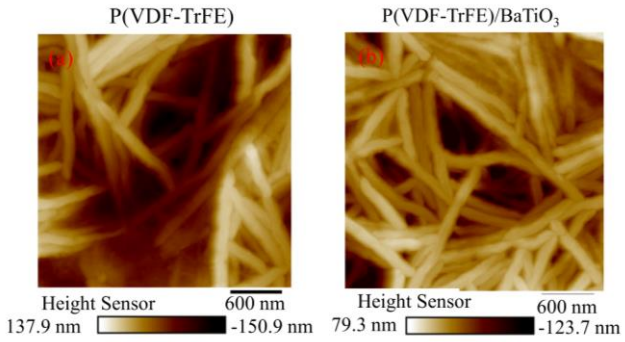

Figure 6: AFM images of P(VDF-TrFE) and P(VDF-TrFE)-BT indicating the emergence of interconnected lamellae upon adding nanoparticles.

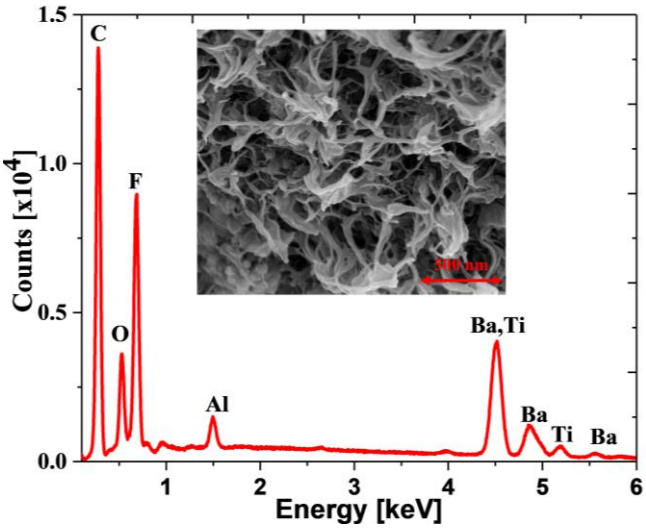

Figure 7: EDX spectra of the nanocomposite highlighting the peaks related to its constituents (inset) SEM images of nanocomposite showing uniform dispersion of BT in P(VDF-TrFE) matrix..

BT NPs were not undergoing any structural deformation in the device processing [19]. In summary, the spectroscopic analysis confirms that the presence of nucleation sites and space charge effect of BT favors the formation of β-phase P(VDF-TrFE).

B. Microscopy characterization

The surface morphology and dispersion state of BT in nanocomposite were studied using Atomic Force Microscopy (AFM) (Fig. 6) and Scanning Electron Microscope (SEM) with EDX analysis (Fig. 7). The AFM images in Fig. 6 predominantly show two types of regions in both P(VDF–TrFE) and P(VDF-TrFE)-BT nanocomposite. In the case of P(VDF-TrFE) (Fig. 6(a)), the notable darker regions correspond to amorphous copolymer state and indicate the nonpolar α phase. In this phase, P(VDF–TrFE) polymer does not exhibit the required ferroelectric response. The lamellar structure in the surface are crystalline fraction of the copolymer. These structures have average length of 1.2 µm and cross-sectional diameter of 0.3 µm and they show the presence of polar β-phase. Macromolecules in β-phase possesses extended long-range order and the adjacent dipoles aid strong intra-dipole interaction. Based on the spectroscopic analysis in previous section and the AFM images it is clear that the addition of

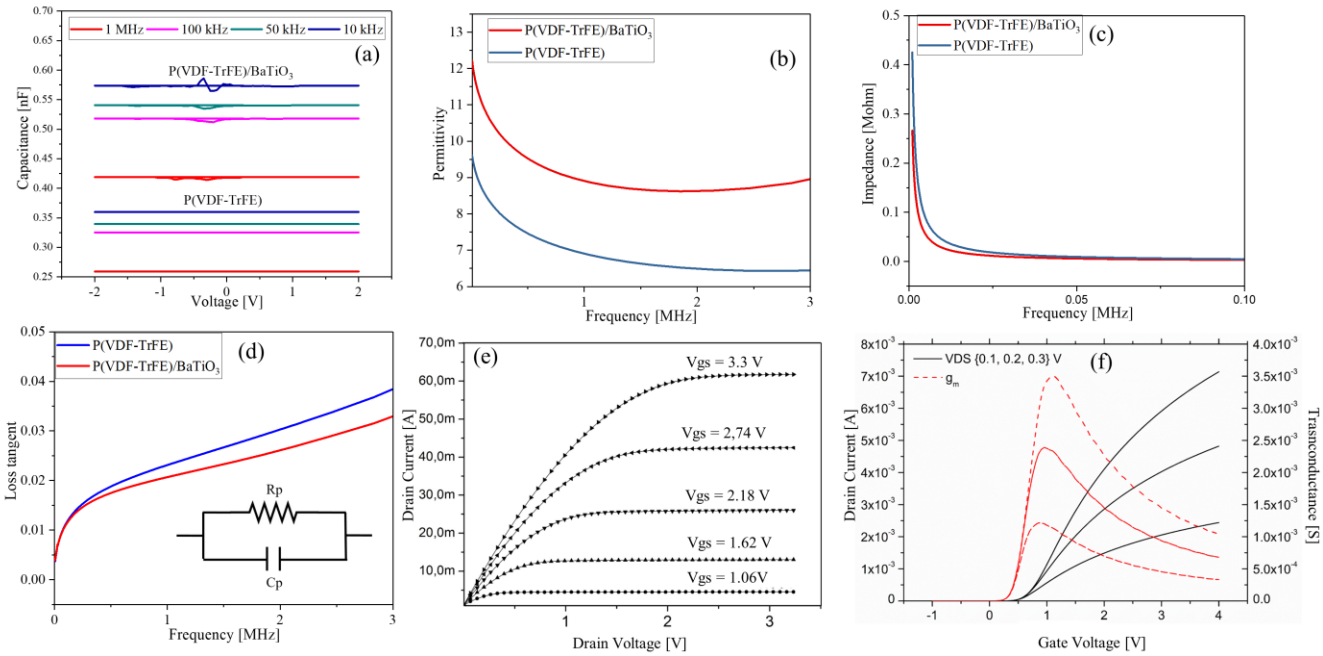

Figure. 8: Electrical characteristics of P(VDF-TrFE)–BT nanocomposite. (a) Capacitance vs Voltage, (b) Dielectric Permittivity vs Frequency (c) Impedance vs Frequency, (d) Loss tangent vs Frequency (e) Output characteristics of FET at different gate voltages, (f) Transfer characteristic of FET at different drain voltages.

ceramic nanoparticles leads to the formation of interconnected lamellar structure in the film. The improved polar β phase shown by these structures aligns with previous reports [39]. The ratio of brighter to darker area, which corresponds to the ratio between polar and nonpolar phase improved significantly in the case of P(VDF-TrFE)-BT. The increase in β-phase is due to the spatial confinement of the polymer chains imposed by the nanoparticles and amplified by charge-dipole interfacial interactions [40]. Moreover, the lamellae average length also increases to 1.5 µm and with reduction in diameter to 0.2 µm that helps to obtain high aspect ratio lamellae.

Extended microscopy analysis was carried through SEM to obtain surface morphology of P(VDF-TrFE)-BT composite. Fig.7(inset) shows the cross-sectional image of the composite with BT NPs dispersed in the matrix. The analysis has been carried out over larger areal coverage to verify the homogeneous dispersion and extended lamellae structure. Additionally, elemental composition of the nanocomposite was determined using SEM-EDX technique (SEM-SU8240). The presence of various elements was confirmed as depicted in Fig. 7. The signal counts are fairly higher to confirm the presence of heavy elements. The observed ratio between Ba and Ti is a good indication of the compound with possible defects. This disturbed stoichiometry keeps the BT NPs positively charged as explained in the spectroscopic measurements. These results show that BT NPs are incorporated in P(VDF-TrFE) matrix during spin coating.

IV. Electrical Characterization And Results

The touch-sensing device was tested for various contact forces and temperatures and the results are presented in this section.

A. *Electrical characterization of nanocomposite and FET*

The dielectric properties such as impedance, loss tangent and permittivity of the nanocomposite were measured with impedance analyser, Summit 12k Autoprober and Keysight B1500A semiconductor parameter analyser. The capacitance-voltage curves shown in Fig. 8(a), obtained at different frequencies (10 kHz, 50 kHz, 100 kHz, 1 MHz), confirm the capacitive behaviour of the structure. The dielectric permittivity was calculated over 1 kHz to 3 MHz frequency range (Fig. 8(b)) using $\varepsilon = \frac{Cd}{A\varepsilon_o}$, and it shows the permittivity enhancement of around 30%. The permittivity enhancement has been used extensively for applications such as energy harvesters and energy storage [17, 18]. The impedances measured over 1-100

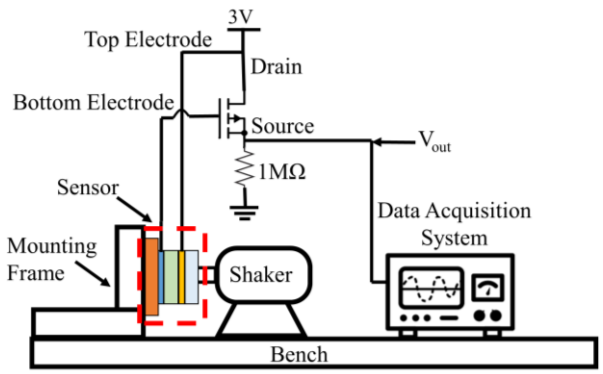

Figure 9: Schematic of characterization setup. Inset shows the experimental setup consisting TIRA shaker.

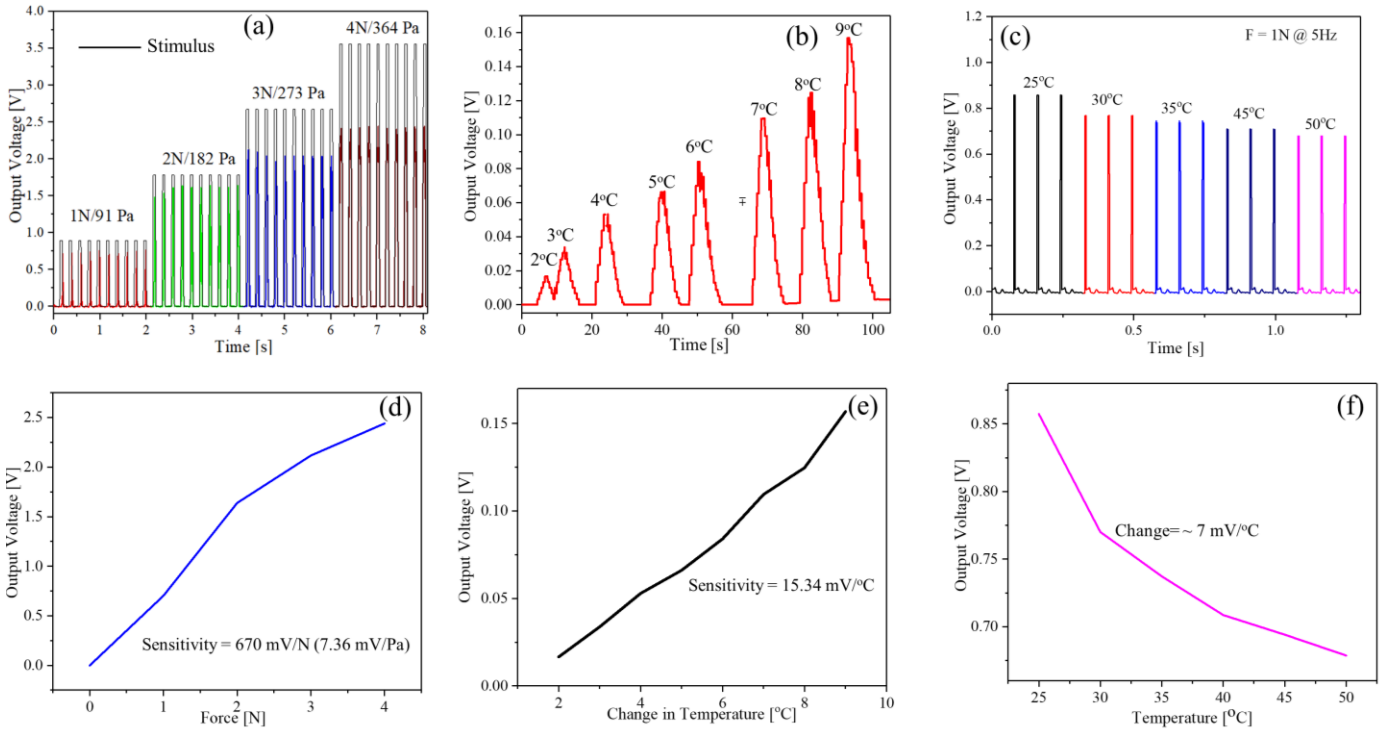

Figure. 10: Force/Pressure and Temperature sensing characteristics of P(VDF-TrFE) –BT based sensor (a) Variation of output voltage at different force/pressure levels (b) Output voltage of sensor with temperature increment (c) Output voltage of sensor at constant force amplitude of 1N and frequency 5 Hz at different temperatures. Calibration curves of P(VDF-TrFE)/BT nanocomposite (d) for variation in force (e) for variation in temperature (f) when both force and temperature vary simultaneously.

kHz does not change much w.r.t. each other, as can be noted from Fig. 8(c). The impedance values for polymer and the nanocomposite merge at ~50 kHz. At higher frequencies, the merging of impedance, suggest that there is a release of space charges which is responsible factor for the enhancement of AC conductivity [41].

The loss tangent was calculated for the frequency up to 3 MHz using $tan\delta = \frac{1}{2\pi f R_p C_p}$, where R_p and C_p are the parallel mode resistance and capacitance of sample. The loss tangent decreases in the P(VDF-TrFE)-BT composites, particularly at higher frequencies as shown in Fig. 8(d). This can be attributed to the glass transition relaxation of the P(VDF-TrFE) polymer matrix [42].

The FET were characterized using 4 probe station and the output characteristics and transfer characteristics are shown in Fig. 8(e) and 8(f). The key device parameters extracted from measured data are threshold voltage, *Vth* = 0.4V, mobility, μ = 705 cm^2/V-s, maximum transconducatnce, g_{max} = 3.5 mS and channel length modulation factor, λ =0.01 V^{-1}.

B. Experimental Results

The experimental setup for mechanical stimulation is shown schematically in Fig.10. It consisted of a rigid frame for mounting the sensor and an electro-mechanical shaker (TIRA model). The sensing structure was placed over the frame and covered with 100 µm thick layer of polydimethylsiloxane (PDMS) for protection during the contact event. The shaker was controlled via a closed loop feedback program to ensure the precise value of force. The tip of shaker was mounted with a piezoelectric force transducer (ICP Force sensor). The tip with the contact area of 0.011 m^2, resulted in force to pressure conversion of 1N → 91 Pa. The sensor was characterized using common-drain or source follower topology, in which the FET's drain terminal and top electrode of sensing layer was biased at 3V. The source of FET was connected to 1MΩ pull-down resistor. The output voltage was recorded across the resistor at varying force magnitude. When a human body comes into contact with the surface of an object the amount of force produced is typically less than 2.0 N and this force can be taken as a center of ballpark area reference for the mechanical stimuli without causing any pain. Moreover, the response time in which a human completes all processing of tactile stimuli from contact detection to response output is 100–200 ms [43]. Therefore, force with magnitude from 1N-4N and frequency 5 Hz was applied. Similarly, temperature range was varied from ambient temperature to 70°C which is the temperature range that is required for most tactile applications [44]. During the sensitivity to temperature measurement, temperature was ramped in step of 1°C from room temperature, so that the difference between two subsequent temperatures was 1°C.

The sensing mechanism can be briefly explained as follow: Upon application of force/temperature, the charge produced in composite due to virtue of piezo/pyroelectricity, modulates the gate voltage of the transistor. The modulated gate voltage in turn changes the drain current, which was measured as change in voltage across the resistor connected at the source terminal. The force level was increased in steps from 1N to 4N, keeping

the frequency constant at 5 Hz. The sensor response to applied force/pressure is shown in Fig.10 (a). The sensitivity measured with this configuration is calculated as 670 mV/N (7.36 mV/Pa) without any extra amplification and shows good linear behaviour to force and without any noticeable hysteresis as shown in Fig.10 (d).

The same configuration was used to sense the change in temperature. For this, the sensing structure was heated gradually with increasing temperature steps (2ºC-9ºC) using hotplate without any mechanical force and the output was recorded as explained previously and shown in Fig.10 (b). This kind of stimulus is similar to common stimulus pattern occurs when a region of one's skin get exposed to a radiant source of heat causing a linear temperature ramp. The sensitivity during this measurement is calculated to be 15.34 mV/ºC and also shows linear behaviour as can be seen from Fig.10 (e).

Table III: Comparison of P(VDF-TrFE)/BaTiO3 sensor with other P(VDF-TrFE) based sensors

	Force Sensitivity (mV/N)	**Temp. Sensitivity (mV/ºC)**	**Ref.**
POSFET	102	12.5	[45]
EG-OFET	65	3.8	[12]
This work	670	15.34	--

To characterize the sensor when force and temperature act together, the sensor was placed in closed chamber. The temperature was increased from 25ºC to 50ºC in step of 5ºC, while a constant force of 1N with frequency 5Hz was applied. The temperature of the sensing layer was recorded from the area which was not covered with protection layer, using an infrared thermometer. As can be observed from Fig. 10 (c), the output voltage slightly decreases as temperature increase, and the decrement was calculated to be around 7mV/ºC as can be seen from Fig.10 (f). This observation shows that charges originating due to pyroelectric effect is in opposite direction to that of due to piezoelectric effect. Comparing the temperature relatedshift with the force/pressure sensitivity of 670 mV/N (7.36 mV/Pa), the temperature effect is negligible while using the presented device as force sensors.

The performance of presented touch sensing devices in compared in Table III with previously reported works based on configuration similar to our device i.e. piezoelectric touch sensing part tightly coupled with FET. In particular, the output is compared with Piezoelectric Oxide Semiconductor Field Effect Transistor (POSFET) and P(VDF-TrFE) coupled with organic FET (OFET). The comparison in Table III clearly shows that the P(VDF-TrFE)-BT nanocomposite-based sensors has better performance.

V. Conclusion

To summarize, 0-3 nanocomposite using P(VDF-TrFE) and $BaTiO_3$ nanoparticles has been used as promising candidate for multimodal tactile sensing. The chosen inclusion enhances the polar phase of matrix as evident from the various studies conducted to analyse the effect of BT addition on the P(VDF-TrFE). FTIR and Raman spectroscopy shows that the nanocomposite exhibits enhanced β phase and AFM analysis reveals higher crystallization. SEM and EDX analysis confirms the uniform dispersion of nanoparticles in the polymer. The dielectric permittivity enhancement and decrease in dielectric loss has also be observed upon addition of BT NPs. The sensitivity of touch-sensing devices to force/pressure is ~670 mV/N/7.36 mV/N and to temperature, it is 15.34 mV/ºC. In the scenario, when both force and temperature act together, the change in output voltage as a result of piezoelectric effect is much higher than the pyroelectric effect. This difference in sensitivities to force and temperature can be further tuned to suitable poling steps to fully decouple the response to force and temperature.

Acknowledgement

Authors are thankful to Dr. Mario Gonzalez Jimenez from Ultrafast Chemical Physics Group of School of Chemistry, University of Glasgow for their support with FTIR analysis. We also acknowledge the support received for this work from James Watt Nanofabrication Centre (JWNC) and Electronics Systems Design Centre (ESDC).

References

[1] C. Bartolozzi, L. Natale, F. Nori, and G. Metta, "Robots with a sense of touch," Nature Mater., vol. 15, p. 921, 2016.

[2] A. Chortos, J. Liu, and Z. Bao, "Pursuing prosthetic electronic skin," Nature Mater., vol. 15, p. 937, 2016.

[3] R. Dahiya and M. Valle, Robotic Tactile Sensing: Technologies and System: Springer, 2013.

[4] N. Yogeswaran, W. Dang, W. T. Navaraj, D. Shakthivel, S. Khan, E. O. Polat, S. Gupta, H. Heidari, M. Kaboli, L. Lorenzelli, G. Cheng, and R. Dahiya, "New materials and advances in making electronic skin for interactive robots," Adv. Robotics, vol. 29, pp. 1359-1373, 2015.

[5] S. Decherchi, P. Gastaldo, R. S. Dahiya, M. Valle, and R. Zunino, "Tactile-data classification of contact materials using computational intelligence," IEEE Trans. Robotics, vol. 27, pp. 635-639, 2011.

[6] C. G. Núñez, W. T. Navaraj, E. O. Polat, and R. Dahiya, "Energy autonomous flexible and transparent tactile skin," Adv. Funct. Mater., vol. 27, p. 1606287, 2017.

[7] R. Dahiya, P. Mittendorfer, M. Valle, G. Cheng, and V. Lumelsky, "Directions Towards Effective Utilization of Tactile Skin - A Review," IEEE Sens. J., vol. 13, pp. 4121 - 4138, 2013.

[8] M. L. Hammock, A. Chortos, B. C. K. Tee, J. B. H. Tok, and Z. Bao, "25th Anniversary Article: The Evolution of Electronic Skin (E-Skin): A Brief History, Design Considerations, and Recent Progress," Adv. Mater., vol. 25, pp. 5997-6038, 2013.

[9] S. Luo, J. Bimbo, R. Dahiya, and H. Liu, "Robotic tactile perception of object properties: A review," Mechatronics, vol. 48, pp. 54-67, 2017.

[10] H. S. Nalwa, Ferroelectric polymers: chemistry: physics, and applications: CRC Press, 1995.

[11] R. Dahiya, A. Adami, L. Pinna, C. Collini, M. Valle, and L. Lorenzelli, "Tactile Sensing Chips With POSFET Array and Integrated Interface Electronics," IEEE Sens. J., vol. 14, pp. 3448-3457, 2014.

[12] S. Hannah, A. Davidson, I. Glesk, D. Uttamchandani, R. Dahiya, and H. Gleskova, "Multifunctional sensor based on organic field-effect transistor and ferroelectric poly (vinylidene fluoride trifluoroethylene)," Organic Electronics, vol. 56, pp. 170-177, 2018.

[13] A. Spanu, L. Pinna, F. Viola, L. Seminara, M. Valle, A. Bonfiglio, and P. Cosseddu, "A high-sensitivity tactile sensor based on piezoelectric polymer PVDF coupled to an ultra-low voltage organic transistor," Organic Electronics, vol. 36, pp. 57-60, 2016.

[14] D. F. Wang, X. Lou, A. Bao, X. Yang, and J. Zhao, "A temperature compensation methodology for piezoelectric based sensor devices," Applied Physics Letters, vol. 111, p. 083502, 2017.

[15] C. Fendzi, M. Rebillat, N. Mechbal, M. Guskov, and G. Coffignal, "A data-driven temperature compensation approach for Structural Health Monitoring using Lamb waves," Structural Health Monitoring, vol. 15, pp. 525-540, 2016.

[16] S. Gupta, L. Lorenzelli, and R. Dahiya, "Multifunctional flexible PVDF-TrFE/BaTiO3 based tactile sensor for touch and temperature monitoring," in IEEE Sensors, Glasgow, 2017, pp. 1-3.

[17] J. Nunes-Pereira, V. Sencadas, V. Correia, J. G. Rocha, and S. Lanceros-Méndez, "Energy harvesting performance of piezoelectric electrospun polymer fibers and polymer/ceramic composites," Sensors and Actuators A: Physical, vol. 196, pp. 55-62, 2013.

[18] Y. Wang, J. Cui, Q. Yuan, Y. Niu, Y. Bai, and H. Wang, "Significantly Enhanced Breakdown Strength and Energy Density in Sandwich‐Structured Barium Titanate/Poly (vinylidene fluoride) Nanocomposites," Adv. Mater., vol. 27, pp. 6658-6663, 2015.

[19] S.-H. Shin, Y.-H. Kim, M. H. Lee, J.-Y. Jung, and J. Nah, "Hemispherically aggregated BaTiO3 nanoparticle composite thin film for high-performance flexible piezoelectric nanogenerator," ACS Nano, vol. 8, pp. 2766-2773, 2014.

[20] N. Joseph, S. K. Singh, R. K. Sirugudu, V. R. K. Murthy, S. Ananthakumar, and M. T. Sebastian, "Effect of silver incorporation into PVDF-barium titanate composites for EMI shielding applications," Materials Research Bulletin, vol. 48, pp. 1681-1687, 2013.

[21] N. R. Alluri, B. Saravanakumar, and S.-J. Kim, "Flexible, Hybrid Piezoelectric Film (BaTi (1–x) Zr x O3)/PVDF Nanogenerator as a Self-Powered Fluid Velocity Sensor," ACS applied materials & interfaces, vol. 7, pp. 9831-9840, 2015.

[22] Y. Rao, S. Ogitani, P. Kohl, and C. Wong, "Novel polymer–ceramic nanocomposite based on high dielectric constant epoxy formula for embedded capacitor application," Journal of Applied Polymer Science, vol. 83, pp. 1084-1090, 2002.

[23] C. Zhang, Q. Chi, J. Dong, Y. Cui, X. Wang, L. Liu, and Q. Lei, "Enhanced dielectric properties of poly (vinylidene fluoride) composites filled with nano iron oxide-deposited barium titanate hybrid particles," Scientific Reports, vol. 6, p. 33508, 2016.

[24] D. C. Arnold, "Composition-driven structural phase transitions in rare-earth-doped BiFeO 3 ceramics: a review," IEEE Trans. Ultrasonics, Ferroelectrics, and Frequency Control, vol. 62, pp. 62-82, 2015.

[25] T. Hanemann and D. V. Szabó, "Polymer-nanoparticle composites: from synthesis to modern applications," Materials, vol. 3, pp. 3468-3517, 2010.

[26] S. Khan, W. Dang, L. Lorenzelli, and R. Dahiya, "Flexible Pressure Sensors Based on Screen-Printed P(VDF-TrFE) and P(VDF-TrFE)/MWCNTs," IEEE Trans. Semiconductor Manufacturing, vol. 28, pp. 486-493, 2015.

[27] B. Ploss, B. Ploss, F. G. Shin, H. L. Chan, and C. Choy, "Pyroelectric or piezoelectric compensated ferroelectric composites," Applied Physics Letters, vol. 76, pp. 2776-2778, 2000.

[28] I. Graz, M. Krause, S. Bauer-Gogonea, S. Bauer, S. P. Lacour, B. Ploss, M. Zirkl, B. Stadlober, and S. Wagner, "Flexible active-matrix cells with selectively poled bifunctional polymer-ceramic nanocomposite for pressure and temperature sensing skin," Journal of Applied Physics, vol. 106, p. 034503, 2009.

[29] M. Krause, I. Graz, S. Bauer-Gogonea, S. Bauer, B. Ploss, M. Zirkl, B. Stadlober, and U. Helbig, "PbTiO3 – P(VDF-TrFE) – Nanocomposites for Pressure and Temperature Sensitive Skin," Ferroelectrics, vol. 419, pp. 23-27, 2011/01/01 2011.

[30] R. Patil, A. Ashwin, and S. Radhakrishnan, "Novel polyaniline/PVDF/BaTiO3 hybrid composites with high piezo-sensitivity," Sensors and Actuators A: Physical, vol. 138, pp. 361-365, 2007.

[31] D. Olmos, G. González-Gaitano, A. Kholkin, and J. González-Benito, "Flexible PVDF-BaTiO3 nanocomposites as potential materials for pressure sensors," Ferroelectrics, vol. 447, pp. 9-18, 2013.

[32] K.-i. Kakimoto, K. Fukata, and H. Ogawa, "Fabrication of fibrous BaTiO3-reinforced PVDF composite sheet for transducer application," Sensors and Actuators A: Physical, vol. 200, pp. 21-25, 2013.

[33] M. J. Hockley, H. H. S. Chang, and Z. Huang, "Pyroelectric coefficient difference under open and short circuit conditions and their enhancements in laminate composites," Journal of Applied Physics, vol. 109, p. 064102, 2011.

[34] Y. Phermpornsakul, S. Muensit, and I. L. Guy, "Determination of piezoelectric and pyroelectric coefficients and thermal diffusivity of 1-3 PZT/epoxy composites," IEEE Transactions on Dielectrics and Electrical Insulation, vol. 11, pp. 280-285, 2004.

[35] J. Gao, D. Xue, W. Liu, C. Zhou, and X. Ren, "Recent Progress on BaTiO3-Based Piezoelectric Ceramics for Actuator Applications," in Actuators, 2017, p. 24.

[36] L. Dong, D. S. Stone, and R. S. Lakes, "Enhanced dielectric and piezoelectric properties of x BaZrO3-(1− x) BaTiO3 ceramics," Journal of Applied Physics, vol. 111, p. 084107, 2012.

[37] A. Bune, C. Zhu, S. Ducharme, L. Blinov, V. Fridkin, S. Palto, N. Petukhova, and S. Yudin, "Piezoelectric and pyroelectric properties of ferroelectric Langmuir–Blodgett polymer films," Journal of Applied Physics, vol. 85, pp. 7869-7873, 1999.

[38] Y. Qi, L. Pan, L. Ma, P. Liao, J. Ge, D. Zhang, Q. Zheng, B. Yu, Y. Tang, and D. Sun, "Investigation on FT-IR spectra and dielectric property of PVDF/inorganic composites," Journal of Materials Science: Materials in Electronics, vol. 24, pp. 1446-1450, 2013.

[39] W. Ma, J. Zhang, B. V. d. Bruggen, and X. Wang, "Formation of an interconnected lamellar structure in PVDF membranes with nanoparticles addition via solid‐liquid thermally induced phase separation," Journal of Applied Polymer Science, vol. 127, pp. 2715-2723, 2013.

[40] K. Al Abdullah, M. A. Batal, R. Hamdan, T. Khalil, J. Zaraket, M. Aillerie, and C. Salame, "The Enhancement of PVDF Pyroelectricity (Pyroelectric Coefficient and Dipole Moment) by Inclusions," Energy Procedia, vol. 119, pp. 545-555, 2017.

[41] Z. Imran, M. Rafiq, and M. Hasan, "Charge carrier transport mechanisms in perovskite CdTiO3 fibers," AIP Advances, vol. 4, p. 067137, 2014.

[42] K. Yu, H. Wang, Y. Zhou, Y. Bai, and Y. Niu, "Enhanced dielectric properties of BaTiO3/poly(vinylidene fluoride) nanocomposites for energy storage applications," Journal of Applied Physics, vol. 113, p. 034105, 2013.

[43] C. T. Morgan, "Response," in Foundations of psychology., ed Hoboken, NJ, US: John Wiley & Sons Inc, 1948, pp. 40-63.

[44] I. Darian-Smith and K. O. Johnson, "Thermal Sensibility and Thermoreceptors," Journal of Investigative Dermatology, vol. 69, pp. 146-153, 1977.

[45] R. Dahiya, D. Cattin, A. Adami, C. Collini, L. Barboni, M. Valle, L. Lorenzelli, R. Oboe, G. Metta, and F. Brunetti, "Towards Tactile Sensing System on Chip for Robotic Applications," IEEE Sens. J., vol. 11, pp. 3216-3226, 2011.

Mr. Shoubhik Gupta received his Bachelor of Technology degree in Electrical Engineering from Indian Institute of Technology Kanpur, India in 2014. He joined Bendable Electronics and Sensing Technologies (BEST) group of Electronics and Nanoscale Division of University of Glasgow, UK in 2014 as PhD student. His current research area is ultra-thin silicon chips and its application in flexible electronics, especially electronic skin. He has authored 22 research articles. He also worked at Fondazione Bruno Kessler, Italy as Early Stage Researcher. He has been recipient of Marie Curie fellowship from European Commission, Nano-Undergraduate Research Fellowship from University of Notre Dame, USA, Principle Early Career Mobility Scholarship and Dr David K Brown scholarship from University of Glasgow. He was a visiting scholar with the University of Notre Dame, USA, and McGill University, Canada.

Dr. Dhayalan Shakthivel is a post-doctoral researcher at the school of engineering, University of Glasgow, UK. He received Ph.D in Materials Science from the Indian Institute of Science (IISc), Bangalore, India. His research interests are synthesis and application of semiconducting nanowires, kinetic studies of nanostructures growth, nanoscale crystal growth, Nano-pattering, electron microscopy, chemical vapor deposition (CVD) and nanowires based flexible electronics. His current research focused on semiconducting nanowires for flexible large area electronics towards e-skin application. He is recipient of government of India-MHRD fellowship for Ph.D research. He also received John Robertson Bequest (2015) award at the University of Glasgow.

Dr. Leandro Lorenzelli received the Laurea degree in electronic engineering from the University of Genoa, Genoa, Italy, in 1994, and the Ph.D. degree in electronics materials and technologies from the University of Trento, Trento, Italy, in 1998. During the Ph.D. course, his research activity concerned the development of electrochemical CMOS-based microsensors. In 1998, he joined the staff of the ITC-IRST Microsystems Division, Trento, and was involved in the realization of microsystems for biomedical, environmental, and agro-food applications. Since 2005, he has been responsible for the Microsystems Technology Research Unit, Fondazione Bruno Kessler, Trento. His main scientific interests are in the processing technologies for both bio-microelectromechanical system and micro-transducers.

Prof. Ravinder Dahiya (S'05, M'09, SM'12) is Professor of Electronics and Nanoengineering in the University of Glasgow, U.K. He is the leader of Bendable Electronics and Sensing Technologies (BEST) research group. His group conducts fundamental and applied research in the multidisciplinary fields of flexible and printable electronics, tactile sensing, electronic skin, robotics and wearable systems. He has authored over 200 research articles, 4 books (including 3 in various stages of publication), and 11 patents (including 7 submitted). He has led several international projects. He is a Distinguished Lecturer of the IEEE Sensors Council and is serving on the editorial boards of the Scientific Report and IEEE SENSORS JOURNAL. He is the Technical Program co-chair of IEEE Sensors 2017 and IEEE Sensors 2018. He holds the prestigious EPSRC Fellowship and received in past the Marie Curie Fellowship and Japanese Monbusho Fellowship. Among several awards he has received, the most recent are 2016 Microelectronic Engineering Young Investigator Award and the 2016 Technical Achievement Award from the IEEE Sensors Council.